

Nonlinear Optical Phenomena in Oxides and Application to a Tunable Coherent Spectrometer*

ROBERT L. BYER

Applied Physics Department, Stanford University, Palo Alto, California

Received July 3, 1974

The material requirements for nonlinear interactions in crystal are reviewed with emphasis on the oxide crystals ADP, LiIO₃ and LiNbO₃. The nonlinearity, transparency, and phasematching properties of these three crystals allows efficient nonlinear interactions over a wide 0.22-4 μm spectral range. The advantages of nonlinear processes for generating tunable coherent radiation are illustrated by a tunable coherent spectrometer based on a 1.06 μm Nd:YAG pumped angle tuned LiNbO₃ parametric oscillator. The 1.4-4 μm parametric oscillator tuning range is extended by second harmonic generation in LiNbO₃, LiIO₃ and sum generation in ADP to 0.22 μm and by mixing in AgGaSe₂ and CdSe to 25 μm . The high energy computer controlled coherent spectrometer is now under construction.

I. Introduction

The first nonlinear optical experiment was conducted in an oxide material in 1961 when Franken et al. generated the second harmonic of a Ruby laser in SiO₂ (1). Since that early experiment nonlinear frequency conversion processes have become an integral part of laser technology. These processes include second harmonic generation, sum and difference frequency generation, and parametric oscillation. The frequency range available by nonlinear conversion processes extends from 0.200 μm in the uv to beyond 100 μm in the ir. It is interesting to note that nonlinear interactions in only three oxide materials, NH₃H₂PO₄(ADP), LiIO₃, and LiNbO₃ allow conversion and generation over the uv visible, and near ir part of this extended spectral range. In this paper, I consider the development and application of these oxide crystals to nonlinear optics. In addition to the material parameters, I discuss the application of these three oxide compounds to the generation of coherent radiation over the 0.22-4.0 μm spectral range. The unique properties of these

crystals in nonlinear interactions allow one to conceive of a widely tunable coherent source. Such a tunable coherent spectrometer is presently being constructed and is described in the third part of this paper.

II. Linear and Nonlinear Optical Properties of Oxide Crystals

A. Material Requirements

Nonlinear crystals must satisfy four criteria if they are to be useful for nonlinear optical applications. These criteria are adequate nonlinearity, optical transparency, proper birefringence for phasematching, and sufficient resistance to optical damage by intense optical irradiation. These properties are briefly discussed in this section and are illustrated by descriptions of ADP, LiIO₃, and LiNbO₃.

1. *Nonlinear susceptibility.* In the early days of nonlinear optics adequate laser power was not always available to take full advantage of the potential conversion efficiency of a nonlinear crystal. Under those circumstances, the highest crystal nonlinearity was a very important factor. Since the late 1960s the situation has changed chiefly due to the avail-

* Invited paper.

ability of well controlled high peak power laser sources at many wavelengths across the uv, visible, and ir spectral regions. Under present circumstances, the crystal nonlinearity becomes only one factor in determining the crystal's potential for nonlinear applications. For example, if more than adequate laser power is available, then the nonlinear conversion efficiency is determined by the maximum incident intensity the crystal can withstand prior to the onset of optical damage.

The second harmonic generation conversion efficiency is given by (2, 3).

$$I_{2\omega}/I_{\omega} = \Gamma^2 l^2 \text{sinc}^2(\Delta kl/2), \quad (1)$$

where $I_{2\omega}$ and I_{ω} are the second harmonic and fundamental intensities, $\Gamma^2 l^2$ is the conversion efficiency factor and

$$\text{sinc}(\Delta kl/2) \equiv [\sin(\Delta kl/2)/(\Delta kl/2)]$$

is the phase velocity synchronism factor. For perfect phasematching $\Delta kl = 0$ and $\text{sinc}(\Delta kl/2) = 1$. Here Δk for second harmonic generation can be written as $\Delta k = k_{2\omega} - 2k_{\omega}$ where $|k| = (2\pi n/\lambda)$ is the wavevector.

In the low conversion efficiency limit the second harmonic generation efficiency, sum and difference generation efficiency, and parametric gain coefficient are equal. In the plane wave limit the conversion efficiency factor is (3, 4)

$$\Gamma^2 l^2 = \frac{2\omega^2 |d_{\text{eff}}|^2 l^2 J_{\omega}}{n^3 c^3 \epsilon_0} \quad (2)$$

in MKS units. Here ω is the fundamental frequency, l the crystal length, n the index of refraction ($n_{\omega} = n_{2\omega}$ at phasematching), c the velocity of light and ϵ_0 the permittivity of free space. The conversion efficiency varies as I_{ω} , the intensity of the fundamental wave, and as d_{eff}^2 the square of the effective nonlinear coefficient. This result holds in the plane wave focusing limit where the intensity $I = P/A$ and the area $A = \pi w^2/2$ with w the Gaussian beam electric field radius.

From Eq. (2) it is evident that we can define a material figure of merit for nonlinear interactions in crystals by

$$M = d^2/n^3. \quad (3)$$

Figure 1 shows this figure of merit vs crystal

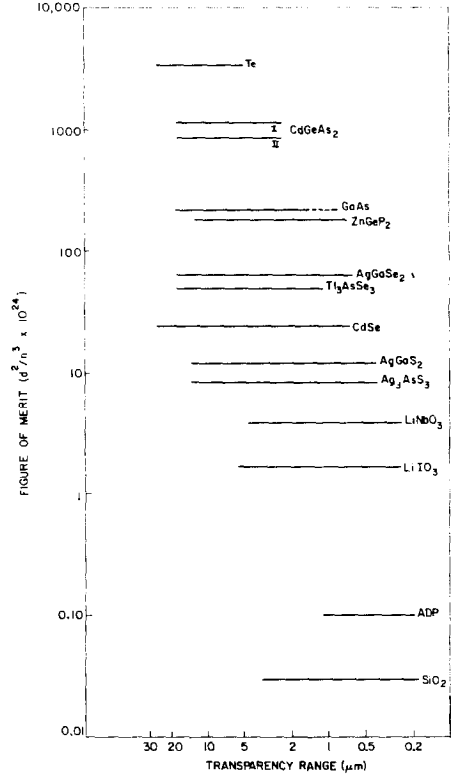


FIG. 1. Nonlinear material figure of merit vs transparency range for nonlinear crystals.

transparency for a number of nonlinear crystals, Inspection of Fig. 1 shows that the oxide materials of interest, ADP, LiIO₃, and LiNbO₃ all have relatively low figure of merits when compared to semiconducting compounds. Fortunately, it is the conversion efficiency factor which is of interest in device applications, and in calculating $\Gamma^2 l^2$, the low material figure of merit for the oxide crystals is compensated by their extended violet and uv transparency range. This suggests that a comparison of $\Gamma^2 l^2$ is more useful. Figure 2 shows $\Gamma^2 l^2$ for nonlinear crystals vs transparency range. The second harmonic wavelength is noted by the tick marks and the $\Gamma^2 l^2$ scaling with λ^2 is indicated. Figure 2 illustrates that whereas M varies over four orders of magnitude, $\Gamma^2 l^2$ is very closely within one order of magnitude for a very wide range of nonlinear crystals including the oxides. Furthermore, for reasonable intensi-

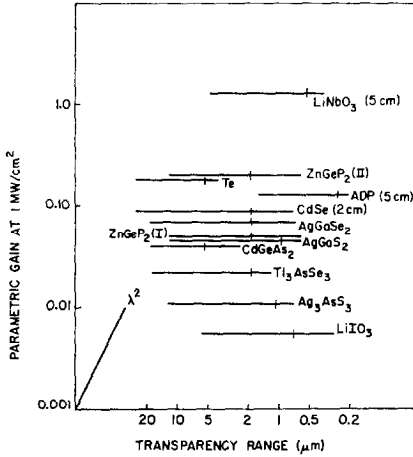


FIG. 2. Second harmonic conversion efficiency (parametric gain) vs transparency at 1 MW/cm² for nonlinear crystals. The crystal length is 1 cm unless indicated. The vertical tick mark indicates the pump wavelength for a parametric oscillator or the second harmonic wavelength for frequency doubling.

ties of less than 10 MW/cm², we can expect $\Gamma^2 I^2 \sim 1$ in most nonlinear materials for only 1 cm of interaction length. Clearly, parameters other than nonlinearity are important in determining the conversion efficiency for a nonlinear process.

Before discussing other material parameters let us return to Eq. (2) to consider the effective nonlinear coefficient d_{eff} . The nonlinear susceptibility is described by an expansion of the polarization in terms of the electric field

$$\mathcal{P} = \epsilon_0 [\chi^{(1)} E + \chi^{(2)} EE + \dots],$$

where $\chi^{(1)}$ is the linear susceptibility and $\chi^{(2)}$ is the nonlinear susceptibility. In addition to satisfying an intrinsic permutation symmetry (5, 6) and Kleinman's symmetry (7), $\chi^{(2)}$ must obey Neumann's Principle and satisfy crystal symmetry as well (8). It is customary to define a nonlinear coefficient $d_{ijk} = d_m$ where m runs from 1 to 6, in a reduced notation, such that

$$\mathcal{P}_i(r, 2\omega) = \epsilon_0 \sum_{m=1}^6 d_{im} [E(r, \omega) E(r, \omega)]_m \times \exp[i2k(\omega) \cdot r],$$

with $\chi_{im}(-2\omega, \omega, \omega) = 2d_{im}(-2\omega, \omega, \omega)$ for

second harmonic generation. The d tensors have the same symmetry as the piezoelectric tensors so that the nonzero components have been listed in tables (8-10).

As an example, the nonlinear d tensor for $\bar{4}2m$ point group to which KDP and its isomorphs belong has the components:

$$\mathcal{P}_x = \epsilon_0 2d_{14} E_y E_z$$

$$\mathcal{P}_y = \epsilon_0 2d_{14} E_x E_z$$

$$\mathcal{P}_z = \epsilon_0 2d_{36} E_x E_y.$$

By Kleinman's symmetry $d_{14} = d_{36}$ so that there is only one value for the nonlinear coefficient. A close look at the form of the tensor components shows that to maximize the nonlinear interaction in KDP type crystals, the field should propagate in a $[110]$ direction. Furthermore, to achieve phasematching for negative uniaxial KDP ($n_e < n_o$) the propagation direction should be at an angle θ with respect to the crystal optic axis such that $n^2(\theta) = n_o^2$. At this propagation direction, the projection of the polarization and electric fields leads to an effective nonlinear coefficient $d_{\text{eff}} = d \sin \theta \sin 2\phi$. Effective nonlinear coefficients have been listed for other crystal classes (11, 12). The effective nonlinear coefficient for LiIO₃ is $d_{\text{eff}} = d \sin \theta$. However, for LiNbO₃ we find

$$d_{\text{eff}} = d_{31} \sin \theta + d_{22} \cos \theta \sin 3\phi.$$

A measurement for LiNbO₃ shows that d_{31} and d_{22} have opposite signs so that d_{eff} is maximum for propagation in the negative yz quadrant. A consideration of d_{eff} is important for both the orientation of a nonlinear crystal and for the growth of crystals to satisfy particular phasematching requirements.

2. *Transparency and optical quality.* Known nonlinear materials have transparency ranges that extend from 0.220 μm in ADP through the ir in a number of semiconductor compounds and beyond the reststrahl band into the far ir in both oxide and semiconductor crystals. In general, the transparency range in a single material is limited by the band edge absorption at high frequencies and by two-phonon absorption at twice the reststrahl band at low frequencies. Materials are also transparent in the very low frequency range between

dc and the first crystal vibrational mode. Thus, nonlinear interactions may extend from the uv through the visible and ir to the far ir. In fact, only a few crystals having the proper birefringence and overlapping transparency ranges are needed to cover the entire extended frequency range. This is important because the growth of high optical quality nonlinear crystals is, in general, a difficult task. In addition, nonlinear crystals that can be grown well, are transparent, and have proper birefringence for phasematching are very rare among all known acentric crystals (14). For example, among 13 000 surveyed crystals, only 684 are uniaxial and phasematchable or 5.25%, and of these less than half have a nonlinearity greater than KDP and far fewer are amenable to crystal growth in high optical quality centimeter sizes.

The transmission loss in a nonlinear crystal reduces the SHG conversion efficiency by $e^{-(\alpha_2/2+\alpha_1)l}$ where α_2 and α_1 are the loss per length at the second harmonic and fundamental waves. Thus, a 0.05 cm^{-1} and 0.025 cm^{-1} loss at 2ω and ω in a 1 cm long crystal reduces the SHG efficiency by 0.95 which is negligible. However, in a 5 cm crystal the same losses reduce the efficiency by 0.77, which is significant. High optical quality oxide materials have losses in the 10^{-3} – 10^{-5} cm^{-1} range, whereas semiconductor materials show much higher losses in the 1 – 10^{-2} cm^{-1} range. The reduction of optical loss in nonlinear crystals is important if the nonlinear interaction is to proceed efficiently. It becomes even more important for operation of a parametric oscillator where the threshold pumping power and operating efficiency directly depend on the crystal and cavity losses.

Recently, intensity dependent losses have been recognized as important factors in the transparency of a crystal. At the short wavelength end of a material's transparency range, two-photon absorption may become the dominant loss mechanism even in a frequency range that is normally transparent to low intensity radiation. For example, at 10 MW/cm^2 the two-photon absorption in GaAs at $1.32 \mu\text{m}$ is 0.3 cm^{-1} , which is significant compared to the 0.05 cm^{-1} normal absorption loss (15). This nonlinear absorption

mechanism has also been observed in oxide nonlinear materials for intense pump radiation within the two-photon frequency range of the band edge. Thus for maximum efficiency pump wavelengths must be longer than the two-photon absorption edge of the nonlinear crystal although operation near the band edge is possible at lower efficiencies and pump intensities.

The two-photon absorption limit was in mind when pump wavelengths for the parametric gain calculations shown in Fig. 2 were chosen.

3. Birefringence and phasematching. For efficient nonlinear interactions phasematching must be achieved in the nonlinear crystal. As an example, SHG in cubic crystals that lack birefringence and thus are not phase-matchable, occurs only over a distance of one coherence length between 10 and $100 \mu\text{m}$. By using birefringence to offset dispersion, the phasematched interaction may proceed over the full crystal length or approximately 1 cm. Since the SHG efficiency varies as l^2 , phasematching increases the efficiency by at least 10^4 . The enormous improvement in nonlinear conversion efficiency due to phasematching makes phasematching essential in nonlinear crystals. Thus, if a crystal is nonlinear and transparent, it must still phasematch to be useful. Adequate birefringence for phasematching is the most restrictive requirement placed on a nonlinear crystal.

In conducting surveys for new nonlinear crystals, the crystal symmetry is determined by X-ray methods or by reference to existing tables (16). If the crystal is acentric and belongs to a point group that gives nonzero nonlinear coefficients for phasematching (17), then the crystal indices of refraction and birefringence must be determined. Fortunately, mineralogy texts and data collections are available (18) which list indices of refraction and birefringence for a large number of crystals. A comparison of the crystal birefringence against its index of refraction and similar quantities for known phase-matchable crystals gives a quick indication of whether the potential nonlinear crystal has adequate birefringence for phasematching, Wemple (19), Wemple and DiDomenico (20), and Byer (14) have plotted

birefringence vs index of refraction for known nonlinear crystals to determine the minimum required birefringence for phasematching. Such plots are useful, since birefringence of a particular crystal cannot accurately be determined theoretically at this time.

Of course the above preliminary indications of possible phasematching in a new material must be carried a step further to determine the actual phasematching properties of a crystal. This is usually done by accurately measuring the crystal indices of refraction and fitting the results to an analytical expression which is useful for phasematching calculations. The measurement of crystal indices of refraction is tedious experimentally, especially in the ir, so that complete measurements have been made on only a few crystals (9, 10). The measurements must be accurate to 0.01% for phasematching calculations to be made. For calculation purposes, the index values vs wavelength are usually expressed by a Sellmeier equation or modified Sellmeier equation. Once in this form, the phasematching expression for SHG $n_o^\omega = n_e^{2\omega}(\theta)$ can be solved directly for the phasematching angle θ . For three-frequency phasematching conditions, a small computer program is usually written to solve simultaneously the two equations $\omega_3 = \omega_2 + \omega_1$ and $k_3 = k_2 + k_1$, where $k = 2\pi n(\lambda)/\lambda$. Care must be taken in solving these equations since they may be double valued. The LiNbO₃ parametric oscillator tuning curves shown in Fig. 3 were calculated in this manner using analytical expressions for the index of refraction given by Hobden and Warner (21).

Nonlinear crystals must also have a very uniform birefringence over the crystal length for efficient nonlinear conversion. In early stages of crystal growth birefringence variations may be a result of composition changes during growth. For example, early stoichiometrically grown LiNbO₃ crystals had birefringence variations which reduced their overall quality (22-25). The problem was fully solved by growth of LiNbO₃ from a congruent melt composition near a lithium to niobium ratio of 0.48 mole % (26, 27). The growth of LiNbO₃ crystals from a congruent melt plus improved optical tests for birefringence uni-

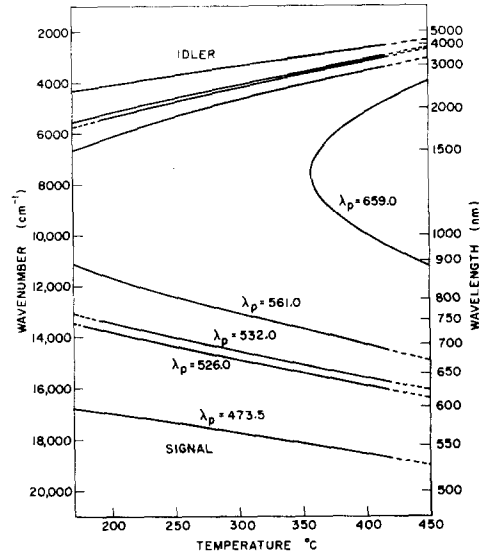


FIG. 3. Temperature tuned LiNbO₃ parametric oscillator tuning curves for various pump wavelengths of a doubled Nd:YAG Q-switched laser source.

formity (24, 28, 29) led to uniform high quality single crystals of over 5 cm in length.

Another limitation to nonlinear conversion efficiency is the breaking of phasematching due to thermally induced birefringence changes. This problem has been treated in detail for SHG by Okada and Ieiri (30). They show that the optimum phasematching temperature shifts with increasing average laser power. In crystals with a large birefringence change with temperature such as ADP and LiNbO₃, thermal breaking of phasematching becomes serious at average power levels near 1 W. On the other hand, crystals such as LiIO₃ which have a small temperature variation of birefringence can handle much higher average powers.

4. *Damage intensity.* An important limitation to the maximum nonlinear conversion efficiency is crystal damage due to the input laser intensity. Laser induced damage may be the result of a number of interactions in the material. Ready (31) discusses possible damage mechanisms in a monograph on the effects of high power laser radiation. Among the mechanisms considered are thermal heating, induced absorption due to multiphoton absorption which leads to heating or to breakdown, stimulated Brillouin scattering, self-

focusing, surface preparation, and dielectric breakdown. Thermal heating, in which the temperature rise of the material is proportional to the input pulse duration or deposited energy is a common damage mechanism in metals and highly absorbing materials. Semiconductors behave more like metals than dielectrics for this form of damage.

Damage thresholds for dielectric materials are generally much higher than for semiconductors. For example, sapphire damages near 25 GW/cm^2 for Q -switch pulse irradiation. Glass and Guenther (32) have reviewed damage studies in dielectrics. They point out that nonlinear materials show a marked decrease in damage threshold for phase-matched second harmonic generation. For example, LiIO_3 shows surface damage at 400 MW/cm^2 for 10 nsec pulses. When phase-matched it damages at 30 MW/cm^2 for the fundamental and 15 MW/cm^2 for the second harmonic. Similar results have been noted in LiNbO_3 and $\text{Ba}_2\text{NaNb}_5\text{O}_{15}$.

Bass and Barrett (33) proposed a probabilistic model for laser induced damage based on an avalanche breakdown model. For this damage mechanism, the laser field acts as an ac analogue to dc dielectric breakdown. A laser power density of 10 GW/cm^2 corresponds to $4 \times 10^6 \text{ V/cm}$ which is close to the measured dc dielectric breakdown fields near $30 \times 10^6 \text{ V/cm}$. Bass and Barrett (33) have presented the laser damage threshold in a probabilistic way such that the probability to induce damage is proportional to $\exp(-K/E)$ where K is a constant and E is the rms optical field strength. Measured dielectric breakdown intensities lie near 25 GW/cm^2 for glasses and fused silica and between 2 and 4 GW/cm^2 for nonlinear crystals. It appears that if other damage mechanisms do not limit the laser intensity to lower levels, then laser induced dielectric breakdown determines the maximum incident intensity. Efforts to understand the mechanisms of laser induced damage have been increasing (34, 35). Hopefully these studies will lead to a better understanding of the material's damage intensity limits.

Fortunately, the damage intensity for most nonlinear materials lies between 10 MW/cm^2 and 1 GW/cm^2 . Figure 2 then shows that

nonlinear conversion efficiencies or parametric gains are high for crystal lengths on the order of 1 cm. The damage intensity does place a limit on the energy handling capabilities of nonlinear crystals. Thus, Q -switched laser pulses energies transmitted through 1 cm^2 area crystals are limited to 1–10 J. For most applications of nonlinear crystals, this is not a serious limit since the laser host medium and the nonlinear material damage at similar beam intensities.

B. Oxide Crystals

1. *KDP and its isomorphs* KDP, ADP, and their isomorphs are ferroelectric crystals (36) belonging to the $42m$ tetragonal point group above their Curie temperatures. The KDP crystals are transparent from 0.21 to $1.4 \mu\text{m}$ for the nondeuterated and 0.21 – $1.7 \mu\text{m}$ for the deuterated material (37). ADP has a similar transparency range. KDP and its isomorphs are negative birefringent and are phase-matchable over most of their transparency range. Over small regions of wavelength the crystals 90° phase-match with temperature as the variable. For a complete reference to crystal indices of refraction see Milek and Wells (37), Bechmann and Kurtz (9), and Singh (10).

Because of the availability of large, high optical quality crystals, KDP and ADP were the subject of early nonlinear optical experiments by Miller (38, 39). Later Francois (40) and Bjorkholm and Siegman (41) made accurate *cw* measurements of ADP's nonlinearity. In addition, Bjorkholm (32) has made comparative nonlinear coefficient measurements of other crystals relative to KDP and ADP.

Parametric amplification was first reported by Wang and Racette (43) in ADP. Their report was closely followed by reports of parametric gain in KDP and ADP by Akhmanov et al. (44). In 1966, Akhmanov et al. (45) achieved parametric oscillation in KDP pumped by $0.53 \mu\text{m}$ from a KDP doubled Nd:Glass laser. That work was extended to the demonstration of parametric superfluorescence in a multipass traveling wave oscillator using ADP and KDP (46).

Recently, Yarborough and Massey (47) used the fourth harmonic of a Nd:YAG laser to generate high gain parametric

oscillation in ADP. This high gain oscillator generated 100 kW peak power and 10 mW average power output across the visible spectrum. Overall average power conversion from the 1.06 Nd:YAG source to the uv was 5.3% yielding an average power of 30 mW at 30 pps at 0.2662 μm . The peak uv power was 200 kW and the power density at the ADP generator crystal was 750 MW/cm².

KDP and ADP have played a significant role as efficient second harmonic generators for both cw and pulsed sources. For cw doubling ADP and KDP can be temperature tuned to the 90° phasematching condition over a limited range of fundamental wavelengths between 0.54 and 0.49 μm at temperatures between +60 and -80°C (48, 49). In particular ADP and KDP 90° phasematch for doubling 5145 Å at -9.2 and -11.0°C. Other isomorphs of KDP 90° phasematch over different wavelength regions. For example, rubidium dihydrogen arsenate (RDA) 90° phasematches for doubling the 0.694 μm Ruby laser and cesium, dihydrogen arsenate (CDA) 90° phasematches for doubling 1.06 μm (50). Using 90° phasematched ADP, Dowley and Hodges (48) obtained up to 100 mW of 0.2573 μm in 1 msec pulses and 30–50 mW of cw power. The doubling was performed internal to an argon ion laser cavity to take advantage of the high circulating fields. The SHG efficiency was strongly dependent on crystal losses.

The uv transparency and phasematching characteristics of KDP isomorph crystals make them useful for uv generation by sum and second harmonic generation. Huth et al., (51), were the first to demonstrate this capability by externally doubling a dye laser source. Similarly, Yeung and Moore (52) and Sato (53) have generated tunable uv between 0.3044 and 0.3272 μm by summing a Ruby pumped dye laser and a Ruby laser. Wallace (54) reported an intracavity doubled dye laser that tunes between 0.2610 and 0.3150 μm . This source uses a Q-switched internally doubled Nd:YAG laser as a pump source for the rhodamine 6G and sodium fluorescein dye laser. The KDP intracavity doubled dye laser produced 32 mW of average power at

0.2900 μm in a 2–3 cm⁻¹ bandwidth. The conversion efficiency from input doubled Nd:YAG to uv power was 4.3%. At the 65° phasematching angle used for doubling the rhodamine 6G dye laser, ADP has a conversion efficiency to the second harmonic of 1% per 100 W of input power.

Recently, Massey (55) has shown that the fifth harmonic of 1.06 μm can be phasematched for sum generation in ADP. In addition, using a tunable source between 0.2460 and 0.3270 μm summed with 1.06 μm in ADP, wavelengths between 0.2500 and 0.2000 μm can be generated. This represents the shortest wavelengths that can be generated in a nonlinear crystal.

The optical quality and energy handling capability of KDP isomorphs is best illustrated by the work of Yarborough (56) and recently Falk and Ammann (57). Using a 10 pps, 1 J per pulse, Nd:YAG source, 45% efficient doubling to 0.5320 μm has been demonstrated in 90° phasematched 2 cm long CD*A crystal at a phasematching temperature of 103°C. The generated green output has been doubled again in ADP also 90° phasematched with 22% efficiency to generate 100 mJ pulses at 0.2660 μm . The harmonic generation in both CD*A and ADP takes place without damage to the crystals. The output has been used to pump a dye laser with up to 50% conversion efficiency.

The high energy, high average power doubling experiments illustrate the optical quality of KDP and its isomorphs. In addition, the use of 90° phasematching for efficient second harmonic generation demonstrates its advantage in these experiments. Although KDP type crystals have not been utilized extensively in parametric oscillator studies, they play an important role in generating tunable uv radiation by second harmonic and sum generation of tunable visible sources.

2. *LiNbO₃*. LiNbO₃ is a ferroelectric material (58) with a Curie temperature approximately 40°C below its melting point of 1253°C. Since the recognition of the unique electro-optical (59) and nonlinear optical (60) properties of LiNbO₃ in 1964, it has been extensively studied. The growth and physical

properties of LiNbO_3 have been discussed in a series of papers by Nassau et al. (61), and by Abrahams et al (62). The electro-optical coefficients for LiNbO_3 have been measured by a number of workers (63–67) as have the indices of refraction (68, 69). A particularly useful form for the refractive indices, including temperature dependence, is given by Hobden and Warner (21).

Early work with LiNbO_3 showed two potentially troublesome optical properties; optically induced inhomogeneities in the refractive index (70–72) and growth dependent birefringent variations (22–25). The optically induced index inhomogeneities were found to be self annealing for crystal temperatures above approximately 180°C for visible radiation and 100°C for near ir radiation. Attempts to eliminate the induced index inhomogeneities have not been successful, so that LiNbO_3 parametric oscillators usually operate above 180°C . The growth dependent birefringent variations were eliminated by growth of LiNbO_3 from its congruent melting composition near a lithium to niobium ratio of 0.48 mole % (26, 27). The growth of LiNbO_3 crystals from a congruent melt plus improved optical quality tests (24–28) led to uniform high quality *a* and *b* axis single crystals of over 5 cm in length.

Ferroelectric LiNbO_3 has a large variation of birefringence with temperature. This allows SHG at 90° phasematching for fundamental wavelengths between 1 and $3.8\ \mu\text{m}$ at temperature between 0 and 550°C . Conversely, LiNbO_3 90° phasematches for parametric oscillation for a number of pump wavelengths and can be temperature tuned over a broad spectral region. Figure 3 shows the parametric oscillator tuning curves for various pump wavelengths of an internally doubled *Q*-switched Nd:YAG laser. These LiNbO_3 phasematching curves were calculated by using the Hobden and Warner (21) index of refraction expressions. Additional LiNbO_3 tuning curves, including angular dependence, are given by Harris (2) and Ammann et al. (73).

The internally doubled *Q*-switched Nd:YAG pumped LiNbO_3 parametric oscillator is the best developed parametric oscillator at

this time. This system is described by Wallace (74). The Nd:YAG pump laser operates with an internal LiIO_3 doubling crystal, acousto-optic *Q*-switch and two Brewster angle prisms for wavelength selection. The combination of four doubled Nd:YAG pump wavelengths and temperature tuning allows the oscillator to cover the $0.54\text{--}3.65\ \mu\text{m}$ spectral region.

Threshold for the LiNbO_3 parametric oscillator with a 5 cm long 90° phasematched crystal is typically between 300 and 600 W. The peak power conversion efficiency is near 50% for an oscillator operating a few times above the threshold. Due to the finite pump pulse width and oscillator build up time, the energy conversion efficiency is approximately 30%. However, much higher conversion efficiencies have been reported.

The parametric oscillator can be continuously tuned at between 2 and $10\ \text{cm}^{-1}/\text{min}$ by scanning the oven temperature at $1^\circ\text{C}/\text{min}$. This tuning rate may be slow for some applications, but at $0.2\ \text{cm}^{-1}$ bandwidth for the resonant wave it is quite rapid tuning for a pulsed tunable source. There are now over 50 LiNbO_3 parametric oscillators in use. The properties of parametric oscillators are discussed in detail in reviews by Harris (2), Smith (75) and Byer (3).

LiNbO_3 is one of the highest quality nonlinear optical materials. Its use in parametric oscillators to generate tunable radiation over the $0.6\text{--}3.5\ \mu\text{m}$ spectral range is a demonstration of its importance as a nonlinear material.

3. LiIO_3 . In 1968, Kurtz and Perry (76) applied a technique based on the measurement of SHG of powders to the search for nonlinear materials. That search led to the evaluation of α -iodic acid ($\alpha\text{-HIO}_3$) for phasematched second harmonic generation (77). Measurement of the nonlinearity of $\alpha\text{-HIO}_3$ showed that it had a nonlinear coefficient approximately equal to that of LiNbO_3 . The favorable nonlinear properties of $\alpha\text{-HIO}_3$ led to consideration of other AIO_3 crystals (78). One of the first crystals considered was lithium iodate, LiIO_3 . Its optical and nonlinear optical properties were studied by Nath and Haussuhl (79) and Nash et al. (80). The more

favorable optical quality of LiIO_3 compared to $\alpha\text{-HIO}_3$ has led to its use in a number of nonlinear applications spanning its entire transparency range from 0.35 to 5.5 μm .

LiIO_3 (point group 6) has a measured nonlinear coefficient slightly greater than that of LiNbO_3 (42, 81–83). Its indices of refraction and large birefringence ($\Delta n = 0.15$) have been measured as have phasematching angles for various pump wavelengths. LiIO_3 phase-matches at 52° for doubling 0.6943 μm of a Ruby laser (84) and at 30° for doubling a 1.06 μm Nd:YAG laser.

LiIO_3 has proved particularly useful as a high optical quality nonlinear crystal for internal second harmonic generation of a Nd:YAG laser. For this application the laser mirrors are highly reflecting in the infrared but are transparent at the second harmonic. To obtain efficient doubling the laser operates Q -switched. In this mode, the LiIO_3 acts as a nonlinear output coupler and efficiently doubles the Nd:YAG. By operating with a prism in the laser cavity any one of 15 Nd:YAG laser lines can be selected and efficiently doubled by rotating the LiIO_3 to the phasematching angle. In this way wavelengths at 0.473, 0.532, 0.579, and 0.659 μm can be generated. For example, peak powers of over 10 kW and average powers of greater than 1 W have been obtained from the internally doubled Nd:YAG laser source.

In 1970 Campillo and Tang (81) studied spontaneous parametric scattering in LiIO_3 and Dobrzanski et al. (85) carried out similar measurements in a $\alpha\text{-HIO}_2$. Shortly afterward, Goldberg (86) constructed a LiIO_3 parametric oscillator pumped with a Ruby laser and Izrailenko et al. (87) demonstrated an oscillator using LiIO_3 and $\alpha\text{-HIO}_3$ pumped by a doubled Nd:Glass laser.

The LiIO_3 oscillator can be compared with an off angle phasematched LiNbO_3 oscillator. For equal loss and crystal lengths and $\theta = 50^\circ$ for LiNbO_3 the ratio of the oscillator gains is $\Gamma^2 I^2(\text{LiNbO}_3) / \Gamma^2 I^2(\text{LiIO}_3) \approx 3.6$. The LiIO_3 oscillator compares favorably to LiNbO_3 due to its higher damage intensity of 125 MW/cm² compared to approximately 80 MW/cm² for LiNbO_3 . However, LiIO_3 does suffer from internal damage due to inclusions that may

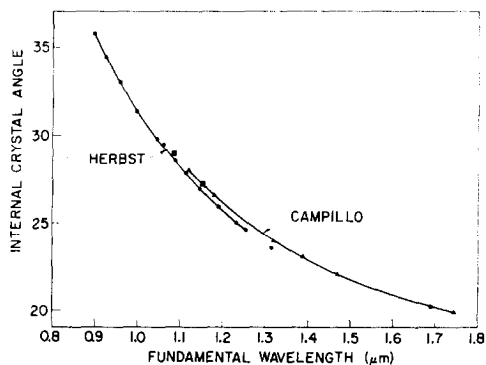


FIG. 4. LiIO_3 second harmonic phasematching angles (double angle) vs wavelength.

occur at lower intensities than for the surface damage.

Campillo (88) also externally doubled the LiIO_3 oscillator using an 8 mm LiIO_3 crystal cut at 21.4° . Figure 4 shows the phasematching angles obtained in that experiment over a range of fundamental wavelengths between 1.1 and 1.8 μm . The second harmonic output at 100 W peak power tuned between 0.560 and 0.915 μm . Figure 4 also shows phasematching data obtained by Herbst (89) in an internally doubled LiNbO_3 parametric oscillator and illustrates the phasematching properties of LiIO_3 for SHG over a broad spectral region.

The ir transmission of LiIO_3 allows interactions out to 5.5 μm . Parametric oscillation is possible but not useful for idler wavelengths this far in the ir due to low gain. However, LiIO_3 does phasematch for mixing. Meltzer and Goldberg (90) have demonstrated mixing in LiIO_3 internal to a Ruby pumped dye laser. Output powers of 100 W were generated over the 4.1–5.2 μm region by mixing the Ruby source with the wavelengths from a DTTC dye laser. The spectral width of the dye laser was 6 \AA in its 0.802–0.835 μm region. Although LiIO_3 is transparent and phasematchable in the near ir spectral region, its low effective nonlinearity, due to the 19° phasematching angle reduces its conversion efficiency to the point that other materials may prove more useful for infrared generation by mixing.

III. A Tunable Coherent Spectrometer

A. Growth of [01.4] LiNbO_3 Boules

Although present LiNbO_3 parametric oscillators are capable of tuning over a wide 0.6–3.5 μm spectral range, they have a number of disadvantages which preclude their use in a well controlled spectrometer. These include: temperature tuning and its disadvantages of slow thermal time constants and lack of direct control, low energy outputs, requirement for mirror changes to cover the full spectral range, and the requirement for visible pump wavelengths from a doubled Q -switched Nd:YAG laser source. The present oscillator does, however, have some significant advantages over other tunable sources. They include: wide tuning range in a single LiNbO_3 crystal, high gain and conversion efficiency, and narrow output bandwidths of less than 30 MHz by the use of internal etalon line narrowing techniques.

We have recently been able to overcome the above disadvantages of the LiNbO_3 parametric oscillator by employing LiNbO_3 crystals fabricated from LiNbO_3 boules grown in the [01.4] direction. The importance of LiNbO_3 boules grown along the [01.4] direction, which lies in the yz plane at 38° to the z axis, is in its application to an angle tuned 1.06 μm pumped high energy LiNbO_3 parametric oscillator described below. First, let me briefly discuss the growth procedure and results.

The requirement for a long (>5 cm) large diameter (>1 cm) high quality LiNbO_3 crystals with an axis direction at 47° to the optic axis for use in an angle tuned 1.06 μm pumped LiNbO_3 parametric oscillator, forced us to consider growing LiNbO_3 along other than the usual y axis direction. Typical y axis boules 8 cm in length by 1.5 cm cross section did not provide enough width to fabricate 47° oriented parametric oscillator crystals of adequate length. Although 1.06 μm parametric oscillators have operated (73, 91), they have not had adequate gain or conversion efficiency due to the limited length of available crystals. To overcome this problem we attempted to grow a boule along the [01.4] growth direction reported by Nassau et al. (61). This direction

was chosen since it maximizes the effective nonlinear coefficient for LiNbO_3 and lies near the desired 47° propagation direction. Figure 5a shows a photograph of a typical [01.4] boule which is over 8 cm in length and 20 mm in diameter. Also shown is a fabricated crystal 5 cm in length and 10 mm diameter operating within a parametric oscillator cavity. The fabricated crystal is very high optical quality, being strain free, striation free and inclusion free over its full volume.

The [01.4] boule was grown in the standard fashion from an oriented (y axis polarity known) seed at the congruent composition. Following growth it was annealed for 24 hr and then poled by applying an electric field along the boule axis. The polarity of the poling field was chosen such that the boule axis was in the negative yz quadrant to maximize the effective nonlinear coefficient. To date 14 boules have been grown without difficulty with typical dimensions of 9 cm \times 25 mm.

In addition to parametric oscillators, the material has been used to fabricate a c axis electro-optic modulator and 35° y -cut LiNbO_3 acoustic transducers. The high optical quality and ease of growth make the [01.4] growth direction preferable for obtaining optical grade LiNbO_3 material.

B. High Energy 1.06 μm Pumped LiNbO_3 Parametric Oscillator

The availability of high quality 5 cm long fabricated crystals in the 47° direction immediately led to the construction of a 1.06 μm pumped angle tuned LiNbO_3 parametric oscillator. The tuning curve for this oscillator is shown in Fig. 6. Figure 6 illustrates a number of potential advantages of this source. First, it is angle tuned which gives the possibility of rapid tuning with full computer control. Second, it has a greater than two-to-one tuning range 1.4 to beyond 4 μm . The oscillator generates two output frequencies within this range, the signal with $\lambda_s < 2.12 \mu\text{m}$ and the idler with $\lambda_i > 2.12 \mu\text{m}$ where 2.12 μm is the degeneracy wavelength. For operation as an oscillator the signal wave only is resonated. This leads to the third advantage of

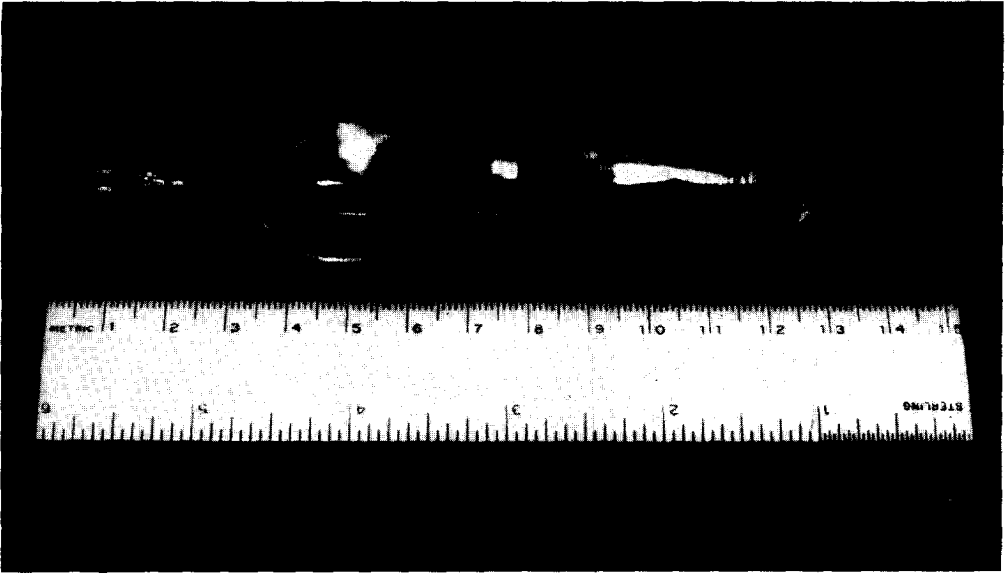


FIG. 5a. Photograph of a [01.4] boule prior to poling

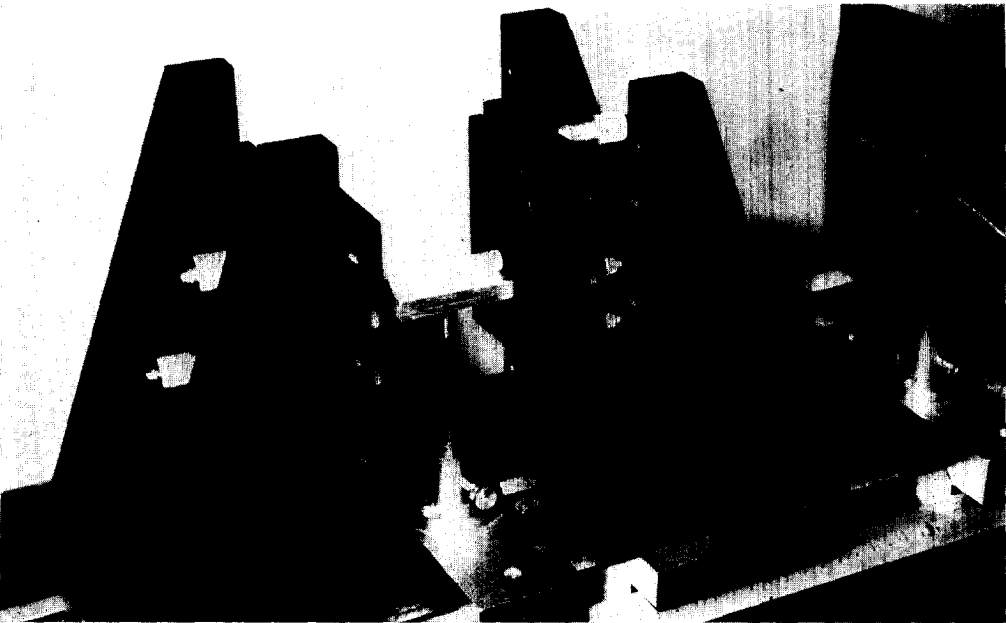


FIG. 5b. Photograph of a fabricated 47° parametric oscillator crystal 5 cm in length by 10 mm diam operating in a $1.06 \mu\text{m}$ pumped parametric oscillator.

this source. Only one set of mirrors are required to obtain the full tuning range of the oscillator so that the optical cavity can be assembled, aligned and permanently sealed. These advantages, along with the previously men-

tioned advantages of high gain and conversion efficiency, and potential operation at very narrow linewidths, make this device a very useful intermediate ir tunable source.

Experimentally we have verified the gain,

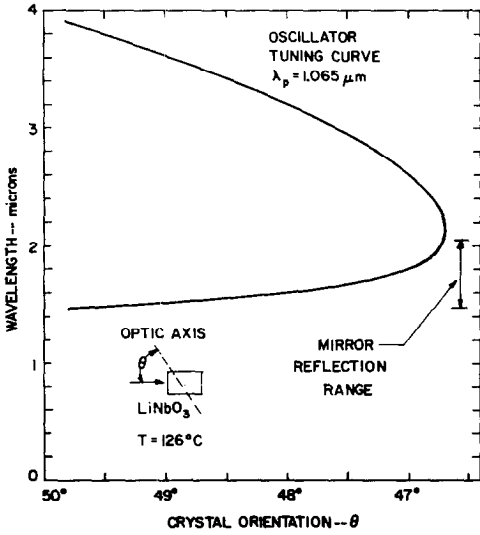


FIG. 6. Angle tuning curve for a 1.06 μm pumped LiNbO_3 parametric oscillator.

conversion efficiency and tuning of the 1.06 μm pumped parametric oscillator. The experiments were carried out using an electro-optic Q -switched 1.06 μm Nd:YAG laser operating at 20 mJ per pulse in a 20 nsec pulse at 10 pps in a TEM_{00} mode. The oscillator operated in a cavity formed by a 2-meter curvature and a flat mirror with the nonantireflection coated LiNbO_3 crystal at room temperature. An energy conversion efficiency of greater than 30% was measured in preliminary experiments. The gain was adequate for oscillation from the crystal surfaces when the resonator was purposely misaligned.

These experiments have confirmed the high optical quality of the [01.4] grown LiNbO_3 boules. The 15 mm diam fabricated crystals allow up to 2 J of 1.06 μm pump energy without exceeding the crystal damage intensity limit. To take advantage of the high energy handling capability of the present crystals, we are presently constructing a Nd:YAG oscillator amplifier system capable of 600 mJ output energy at 10 pps. Based on present laser technology, this 1.06 μm pump laser should operate at near 0.1% efficiency for over 10^7 pulses or 270 hr at 10 pps rate before a flashlamp change is necessary. The high energy LiNbO_3 parametric oscillator forms the heart of a widely tunable coherent

spectrometer with an ultimate tuning range of 0.22 to beyond 25 μm .

C. Extended Frequency Coverage

The angle tuned LiNbO_3 parametric oscillator can be looked at as the central tuning element in a computer controlled widely tunable coherent spectrometer. Its angle tuning and wide 1.5–4 μm tuning range make computer control through stepper motor driven angle stages practical. In addition, its high conversion efficiency and peak output power make further frequency doubling and mixing processes of the primary parametric oscillator wavelengths proceed efficiently. If these doubling and mixing crystals are also angle phasematched and computer controlled, then automatic continuous tuning over an extended range is feasible.

To extend the tuning range toward the visible, the oscillator output is doubled in LiNbO_3 , doubled again in LiIO_3 and finally summed with 1.06 μm in ADP to reach 0.2200 μm . The doubling steps in LiNbO_3 angle phasematch at near 65° to the optic axis has been experimentally measured to have a 52% energy and 70% peak power conversion efficiency. The generated output wavelength from this step covers the 0.75–1.5 μm spectral range.

LiIO_3 phasematches for doubling the 0.75–1.5 μm wavelength range to give 0.375–0.75 μm output. Again, due to the high output powers available, the doubling step is efficient. The tuning range can be further extended into to uv by second harmonic generation in ADP or KDP and by sum generation of 1.06 μm with wavelengths near 0.300 μm . in ADP as recently demonstrated by Massey (55). Wavelengths as short as 0.220 μm can be generated in this manner.

The above frequency doubling steps are angle phasematched so that computer control is possible. The only optics required are polarizers and filters to isolate the generated wavelength of interest. The solid state oxide doubling crystals do not show deterioration with time which is a problem with dye lasers which also provide tunable radiation in this wavelength range.

The parametric oscillator tuning range can

be extended into the infrared by mixing in semiconductor crystals. For this frequency conversion step, the signal and idler of the parametric oscillator are simultaneously incident on the mixing crystal which generates the difference frequency. Phasematching is again achieved by control of the propagation angle within the nonlinear crystal. Mixing in the chalcopyrite AgGaSe_2 (92, 93) phasematches for generation of 3–18 μm wavelengths. Mixing in CdSe (94) phasematches to generate 10–25 μm . Due to the lower optical quality of these semiconductor crystals as compared to the oxide materials, the photon conversion efficiency is expected to be near 10%. However, mixing efficiencies as high as 35% have been observed (94). The output power is further reduced by the Manley–Rowe frequency factor which accounts for the lower energy per photon at the generated infrared output wavelength.

Figure 7 illustrates the tuning range of the LiNbO_3 parametric oscillator as extended by second harmonic generation and mixing. Each tuning range shows the crystal used and the phasematching angle for the process. In all cases except the parametric oscillator,

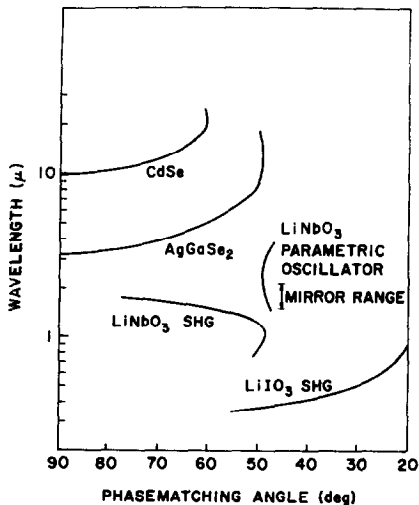


FIG. 7. Extended tuning range of a widely tunable coherent spectrometer. Shown is the output wavelength vs phasematching angle for the LiNbO_3 parametric oscillator and the following doubling and mixing crystals.

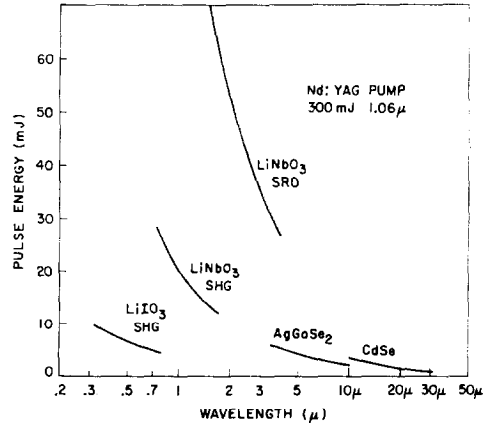


FIG. 8. Predicted output energy per pulse vs wavelength for the high energy tunable source.

two crystals cut at different angles are required to angle phasematch over the full range.

Based on the measured parametric oscillator efficiency and the LiNbO_3 doubling efficiency, and taking a conservative 30% conversion efficiency as practical for the LiNbO_3 parametric oscillator source, we can estimate the expected output energy per pulse vs wavelength. Figure 8 shows such an estimate assuming a 300 mJ per pulse 1.06 μm pump source. The rapid decrease in energy per pulse in the infrared reflects the assumed 10% mixing efficiency and the Manley–Rowe frequency ratio.

IV. Conclusion

Nonlinear interactions in oxide crystals now allow efficient coherent frequency generation over a wide range of the uv, visible, and ir. Progress in the growth and perfection of three oxide crystals, LiNbO_3 , LiIO_3 , and ADP has opened a wavelength range from 0.22 to 4 μm to tunable coherent radiation. The progress in this direction is illustrated by the concept of a widely tunable coherent spectrometer.

Based on a LiNbO_3 parametric oscillator pumped at 1.06 μm and angle tuned over a 1.5–4 μm range, the computer controlled coherent spectrometer utilizes the basic advantages of nonlinear interactions in oxide materials. These include high conversion

efficiency, a wide tuning range for a single crystal, diffraction limited operation, unlimited crystal lifetime and well controlled angle phasematching. Without the combination of these features, unique to nonlinear interactions in crystals, one could not conceive of a computer controlled coherent spectrometer.

The high energy spectrometer is now under construction. Its PDP11/10 minicomputer will act to control the laser source and nonlinear crystal orientations, and will provide real time data handling and display. Initial applications of this unique source include optical pumping spectroscopy, nonlinear spectroscopy and remote air pollution measurements in the ir.

Acknowledgments

I want to acknowledge the crystal growth support provided by R. S. Feigelson of the Stanford Center for Materials Research. I also want to acknowledge the continued assistance of Dr. R. L. Herbst who has carried out much of the design and measurements on the widely tunable coherent source.

This work was partially supported by the Advanced Research Projects Agency through Contract F33615-72-C-2011, by NSF/RANN under subcontract SRI-13851, and by the Honeywell Research Center.

References

1. P. A. FRANKEN, A. E. HILL, C. W. PETERS, AND G. WEINREICH, *Phys. Rev. Letters* **7**, 118 (1961).
2. S. E. HARRIS, *Proc. IEEE* **57**, 2096 (1969).
3. R. L. BYER, Optical parametric oscillators. "Treatise in Quantum Electronics" (H. Rabin and C. L. Tang, Eds.), Academic Press, N.Y., 1974. (To be published.)
4. R. L. BYER, Nonlinear optical phenomenon and materials, *Ann. Rev. Mater. Sci.* **4**, 147 (1974).
5. P. S. PERSHAN, *Phys. Rev.* **130**, 919 (1963).
6. N. BLOEMBERGEN, "Nonlinear Optics" W. A. Benjamin, New York, 1965.
7. D. A. KLEINMAN, *Phys. Rev.* **126**, 1977 (1962).
8. J. F. NYE, "Physical Properties of Crystals." Oxford University Press, London, 1960.
9. R. BECHMANN, AND S. K. KURTZ, "Landolt-Bornstein Numerical Data and Functional Relationships in Science and Technology New Series Group III," Vol. 2. (K. H. Hellwege, Ed.), pp. 167-209. Berlin-Springer Verlag.
10. S. SINGH, Nonlinear optical materials. In "Handbook of Lasers." (R. J. Pressley, Ed.), p. 489. Chemical Rubber Co., Press, Cleveland 1971.
11. G. D. BOYD AND D. A. KLEINMAN, *J. Appl. Phys.* **39**, 3597 (1968).
12. F. ZERNIKE AND J. E. MIDWINTER, "Applied Nonlinear Optics." Academic Press, N.Y., 1973.
13. J. E. BJORKHOLM, *Appl. Phys. Letters* **13**, 36 (1968).
14. R. L. BYER, *Opt. Spectra* **42** (1970).
15. D. A. KLEINMAN, R. C. MILLER, AND W. A. NORDLUND, *Appl. Phys. Letters* **23**, 243 (1973).
16. DONNAY AND DONNAY, "Crystal Data." 2nd ed. American Crystallographic Assoc., 1963.
17. S. K. KURTZ, Nonlinear optical materials. In "Laser Handbook." (F. T. Arecchi and E. O. Schulz, Eds.), pp. 923-974. DuBois North Holland Publishing Company, Amsterdam, Netherlands, 1973.
18. A. N. WINCHELL AND H. WINCHELL, "Optical Properties of Artificial Minerals." Academic Press, N.Y., 1964.
19. S. H. WEMPLE, *Phys. Rev. Letters* **23**, 1156 (1969).
20. S. H. WEMPLE AND M. DiDOMENICO, JR., *J. Appl. Phys.* **40**, 735 (1969).
21. M. V. HOBDEN AND J. WARNER, *Phys. Letters* **22**, 243 (1966).
22. J. G. BERGMAN, A. ASHKIN, A. A. BALLMAN, J. M. DZIEDZIC, H. J. LEVINSTEIN, AND R. G. SMITH, *Appl. Phys. Letters* **12**, 92 (1968).
23. H. FAY, W. J. ALFORD, AND H. M. DESS, *Appl. Phys. Letters* **12**, 89 (1968).
24. J. E. MIDWINTER, *Appl. Phys. Letters* **11**, 128, (1968), see also, J. E. Midwinter, *J. Appl. Phys.* **39**, 3033 (1968).
25. R. C. MILLER, W. A. NORDLUND, AND P. M. BRIDENBAUGH, *J. Appl. Phys.* **42**, 4145 (1971).
26. P. LERNER, C. LEGRAS, AND J. P. DUMAS, Stoechiometrie des monocristaux de Metaniobate de Lithium. In "Crystal Growth," Proceedings of the Second International Conference on Crystal Growth Birmingham, U.K. July 1968. (F. C. Frank, J. B. Mullin and H. S. Peiser, Eds.), p. 231. North Holland Publishing Co., Amsterdam.
27. J. R. CARRUTHERS, G. E. PETERSON, M. GRASSO, AND P. M. BRIDENBAUGH, *J. Appl. Phys.* **42**, 1846, (1971).
28. R. L. BYER, J. F. YOUNG, AND R. S. FEIGELSON, *J. Appl. Phys.* **41**, 2320 (1970).
29. F. R. NASH, G. D. BOYD, M. SARGENT, AND P. M. BRIDENBAUGH, *J. Appl. Phys.* **41**, 2564 (1970).
30. M. OKADA, S. IEIRI, *IEEE J. Quant. Elect.* **QE-7**, 560 (1971).
31. J. F. READY, "Effects of High Power Laser Radiation." Academic Press, N.Y. (1971).
32. A. J. GLASS AND A. H. GUENTHER, *Appl. Optics* **11**, 832 (1972).
33. M. BASS AND H. H. BARRETT, *IEEE J. Quant. Elect.* **QE-8**, 338 (1972).

34. C. R. GIULIANO, *IEEE J. Quant. Elect.* **QE-8**, 749 (1972).
35. M. BASS AND D. W. FRADIN, *IEEE J. Quant. Elect.* **QE-9**, 890 (1973).
36. F. JONA AND G. SHIRANE, "Ferroelectric Crystals." McMilland Co., N.Y., 1962.
37. J. T. MILEK AND S. J. WELLES, "Linear Electro-optic Modulator Materials." Electronic Properties Information Center, Hughes Aircraft Company, (1970).
38. R. C. MILLER, D. A. KLEINMAN, AND A. SAVAGE, *Phys. Rev. Letters* **11**, 146 (1963).
39. R. C. MILLER, *Appl. Phys. Letters* **5**, 17 (1964).
40. G. E. FRANCOIS, *Phys. Rev.* **143**, 597 (1966).
41. G. E. BJORKHOLM AND A. E. SIGEMAN, *Phys. Rev.* **154**, 851 (1967).
42. G. E. BJORKHOLM, *IEEE J. Quant. Elect.* **QE-4**, 970, and correction to above, *IEEE J. Quant. Elect.* **QE-5**, 260 (1968).
43. C. C. WANG AND G. W. RACETTE, *Appl. Phys. Letters* **6**, 169 (1965).
44. S. A. ADHMANOV, A. I. KOVRIGIN, A. S. PISKARSKAS, V. V. FADEEV, AND B. V. KHOKHLOV, *ZhETF Pis. Red.* **2**, 300 [Translation *JETP Letters* **2**, 191 (1965)].
45. S. A. AKHMANOV, A. I. KOVRIGIN, V. A. KILOSOV, A. S. PISKARSKAS, V. V. FADEEV, AND R. V. KHOKHLOV, *JETP Letters* **3**, 241 (1966).
46. A. G. AKHMANOV, S. A. AKHMANOV, R. V. KHOKHLOV, A. I. KOVRIGIN, A. S. PISKARSKAS, AND A. P. SUKHORUKOV, *IEEE J. Quant. Elect.* **QE-4**, 828 (1968).
47. J. M. YARBOROUGH AND G. A. MASSEY, *Appl. Phys. Letters* **18**, 438 (1971).
48. M. W. DOWLEY AND E. B. HODGES, *IEEE J. Quant. Elect.* **QE-4**, 552 (1968).
49. B. G. HUTH AND Y. C. KIANG, *J. Appl. Phys.* **40**, 4976 (1969).
50. R. S. ADHAV AND R. W. WALLACE, *IEEE J. Quant. Elect.* **QE-9**, 854 (1973).
51. B. G. HUTH, G. I. FARMER, L. M. TAYLOR, AND M. R. KAGAN, *Spec. Letters* **1**, 425 (1968).
52. E. S. YEUNG AND C. B. MOORE, *J. Amer. Chem. Soc.* **93**, 2059 (1971).
53. T. SATO, *J. Appl. Phys.* **43**, 1837 (1972).
54. R. W. WALLACE, Generation of tunable UV from 2610 to 3150 Å. *Optics Commun.* **4**, 316 (1971).
55. G. A. MASSEY, *Appl. Phys. Letters* **24**, 371 (1974).
56. J. M. YARBOROUGH. Private communication (1972).
57. J. FALK AND E. O. AMMANN. Private communication (1974).
58. B. T. MATHIAS AND J. P. REINEIKE, *Phys. Rev.* **76**, 1886 (1949).
59. G. E. PETERSON, A. A. BELLMAN, P. V. LENZE, AND P. M. BRIDENBAUGH, *Appl. Phys. Letters* **5**, 62 (1964).
60. G. D. BOYD, R. C. MILLER, K. NASSAU, W. L. BOND, AND A. SAVAGE, *Appl. Phys. Letters* **5**, 234 (1964).
61. K. NASSAU, H. J. LEVINSTEIN, AND G. M. ROIACONO, *J. Phys. Chem. Solids* **27**, 983; *J. Phys. Chem. Solids* **27**, 989 (1966).
62. S. C. ABRAHAMS, J. M. READY, AND J. L. BERNSTEIN, *J. Phys. Chem. Solids* **27**, 997; S. C. ABRAHAMS, W. C. HAMILTON, AND J. M. READY, *J. Phys. Chem. Solids* **27**, 1013; S. C. ABRAHAMS, H. J. LEVINSTEIN, AND J. M. READY, *J. Phys. Chem. Solids* **27**, 1019 (1966).
63. P. V. LENZO, E. G. SPENCER AND K. NASSAU, *J. Opt. Soc. Amer.* **56**, 633 (1966).
64. E. H. TURNER, *Appl. Phys. Letters* **8**, 303 (1966).
65. J. D. ZOOK, D. CHEN, AND G. N. OTTO, *Appl. Phys. Letters* **11**, 159 (1967).
66. K. F. HULME, P. H. DAVIES, AND V. M. COUND, *J. Phys. Chem. (Solid State Phys.)* **2**, 855 (1969).
67. H. KOGELNIK AND T. LI, *Appl. Optics* **5**, 1550 (1966).
68. R. C. MILLER AND A. SAVAGE, *Phys. Rev. Letters* **11**, 146 (1963).
69. G. D. BOYD, W. L. BOND, AND H. L. CARTER, *J. Appl. Phys.* **48**, 1941 (1967).
70. A. ASHKIN, G. D. BOYD, J. M. DZIEDIC, R. G. SMITH, A. A. BALLMAN, J. J. LEVINSTEIN, AND K. NASSAU, *Appl. Phys. Letters* **9**, 72 (1966).
71. F. S. CHEN, *J. Appl. Phys.* **40**, 3389 (1969).
72. W. D. JOHNSTON, JR., *J. Appl. Phys.* **41**, 3279 (1970).
73. E. O. AMMANN, J. D. FOSTER, M. K. OSHMAN, AND J. M. YARBOROUGH, *Appl. Phys. Letters* **15**, 131 (1969).
74. R. W. WALLACE, *Appl. Phys. Letters* **17**, 497 (1970).
75. R. G. SMITH, Optical parametric oscillators. In "Laser Handbook," (F. T. Arecchi and E. O. Schulz-Dubois, Ed.), p. 837. North Holland, Amsterdam, 1972.
76. S. K. KURTZ AND T. T. PERRY, *J. Appl. Phys.* **39**, 3798 (1968).
77. S. K. KURTZ, T. T. PERRY, AND J. G. BERGMAN, JR., *Appl. Phys. Letters* **12**, 186 (1968).
78. J. G. BERGMAN, JR., G. D. BOYD, A. ASHKIN, AND S. K. KURTZ, *J. Appl. Phys.* **40**, 2860 (1969).
79. G. NATH AND S. HAUSSUHL, *Appl. Phys. Letters* **14**, 154 (1969).
80. F. R. NASH, J. G. BERGMAN, JR., G. D. BOYD, AND E. H. TURNER, *J. Appl. Phys.* **40**, 5201 (1969).
81. A. J. CAMPILLO AND C. L. TANG, *Appl. Phys. Letters* **16**, 242, (1970); *Appl. Phys. Letters* **12**, 376 (1968).
82. J. JERPHAGNON, *Appl. Phys. Letters* **16**, 298 (1970).
83. J. E. PEARSON, G. A. EVANS, AND A. YARIV, *Opt. Commun.* **4**, 366 (1972).

84. G. NATH AND S. HAUSSUHL, *Phys. Letters* **29A**, 91 (1969).
85. G. F. DOBRZHANSKII, V. F. KITAeva, L. A. KULESKII, Yu. N. POLIVANOV, S. N. POLUEKTOV, A. M. PROKHOROV, AND N. N. SOBOLOV, *JETP Letters* **12**, 353 (1970).
86. L. S. GOLDBERG, *Appl. Phys. Letters* **17**, 489 (1970).
87. A. I. IZRAILENKO, A. I. KOVRIGIN AND P. V. NIKLES, *JETP Letters* **12**, 331 (1970).
88. A. J. CAMPILLO, *IEEE J. Quant. Elect.* **QE-8**, 809 (1972).
89. R. L. HERBST. Private communication.
90. D. W. METZLER AND L. S. GOLDBERG, *Opt. Commun.* **5**, 209 (1972).
91. J. FALK, J. M. YARBOROUGH, AND E. O. AMMANN, *IEEE J. Quant. Elect.* **QE-7**, 559 (1971).
92. G. D. BOUD, H. M. KASPAR, J. H. MCFEE, AND F. G. STORTZ, *IEEE J. Quant. Elect.* **QE-8**, 900 (1972).
93. R. L. BYER, M. M. CHOY, R. L. HERBST, D. S. CHEMLA, AND R. S. FEIGELSON, *Appl. Phys. Phys. Letters* **24**, 65-68 (1974).
94. R. L. HERBST AND R. L. BYER, *Appl. Phys. Letters* **19**, 527 (1971).